Atmospheric Research 226 (2019) 208–218

Contents lists available at ScienceDirect

Atmospheric Research

journal homepage: www.elsevier.com/locate/atmosres

Synergistic effect of the occurrence of African dust outbreaks on atmospheric pollutant levels in the Madrid metropolitan area

Pedro Salvador[a,*], Francisco Molero[a], Alfonso Javier Fernandez[a], Aurelio Tobías[b], Marco Pandolfi[b], Francisco Javier Gómez-Moreno[a], Marcos Barreiro[a], Noemí Pérez[b], Isabel Martínez Marco[c], María Aránzazu Revuelta[c], Xavier Querol[b], Begoña Artíñano[a]

[a] CIEMAT, Department of Environment, Av. Complutense 40, 28040 Madrid, Spain
[b] Institute of Environmental Assessment and Water Research (IDAEA), CSIC, c. Jordi Girona 18, 08034 Barcelona, Spain
[c] Spanish Meteorological Agency (AEMET), c. Leonardo Prieto Castro 8, 28071 Madrid, Spain

ARTICLE INFO

Keywords:
African dust outbreaks
Mixing layer height
PM_{10}
Health effects

ABSTRACT

The occurrence of African dust outbreaks over specific areas of the Mediterranean basin has been associated with increases in the PM_{10} concentration levels and also in the mortality rates. Different hypothesis have been proposed in the last years to explain the processes by which African dust storms generates negative health effect over urban areas in southern Europe but are still not clear. Some authors have suggested the existence of an interaction between air pollutants from local sources and the occurrence of African dust outbreaks, with a consequent increase in the risk of mortality due to exposure to these anthropogenic emissions. This study sought to identify such a synergistic effect in the Madrid metropolitan area. To this end, an assessment of the influence of African dust on air quality levels, the vertical structure of the atmosphere over Madrid and daily mortality was carried out. Our results indicated that African dust caused a reduction of the mixing layer height and the surface wind speed, by reducing the amount of solar radiation reaching the ground. These facts favored the accumulation of air pollutants emissions from local anthropogenic sources. Moreover, when the dust contribution to PM_{10} levels exceeded a threshold value (8 μg/m^3), particulate matter mass (PM_{10}, $PM_{2.5}$) and number (ultra-fine particles) concentration as well as levels of gaseous air pollutants (CO, NO and NO_2) registered at urban-background and urban-traffic monitoring sites, increased with statistical significance. In these conditions, it was found a statistically significant increase in risk of daily mortality in the PM_{10} exposure. Hence, ambient air in Madrid was more toxic during African dust events of increasing intensity due to this synergistic effect. Because it can be envisaged that the frequency, duration and intensity of dust storms will increase in the north of Africa due to climate change, it will be a priority to put forward and assess proposals to mitigate the adverse effects on health, focused on the reduction of air pollutant emissions from local sources, as well as proposals regarding the adaptation of the population in urban areas across the Mediterranean basin.

1. Introduction

Mineral dust emissions from large arid regions in North Africa depend to a large extent on climate conditions in the source areas, because they drive the annual cycles of dust activity. Dust uptake into the atmosphere is often followed by long range transport towards the Caribbean and southern Europe. These atmospheric transport processes are linked to seasonal changes in large-scale atmospheric circulation patterns (Moulin et al., 1997, 1998; Prospero and Lamb, 2003; Salvador et al., 2014). As a result of the processes of long-range transport, the contributions of African mineral dust registered on the surface can be very highly concentrated in the areas where the dust is deposited. In fact, these types of contributions are the main natural source of PM_{10} (the mass of particulate matter which passes through a size selective impactor inlet with a 50% efficiency cut-off at 10 μm aerodynamic diameter) contributing to the increase of the regional background levels across the Mediterranean basin (Querol et al., 1998, 2009). They also give rise to episodes where the maximum daily value of PM_{10} for the protection of health (set at 50 μg/m^3 in EU Directive 2008/50/EC on ambient air quality and a cleaner atmosphere in Europe) is exceeded in regional and urban air quality monitoring stations (Escudero et al., 2007a; Pey et al., 2013; Salvador et al., 2013 among others).

* Corresponding author.
E-mail address: pedro.salvador@ciemat.es (P. Salvador).

https://doi.org/10.1016/j.atmosres.2019.04.025
Received 27 December 2018; Received in revised form 28 February 2019; Accepted 23 April 2019
Available online 24 April 2019

It has also been demonstrated that African dust produces adverse effects on health, including increases in mortality rates in Southern Europe (Staffogia et al., 2016 and references therein) and specifically in many Spanish regions (Tobías et al., 2011; Pérez et al., 2012a; Díaz et al., 2017). The mechanisms that produce the adverse effects on health during these events are still not clear. It has been proposed that the air masses that carry the mineral dust can also transport biogenic matter (pollen, bacteria, fungi and endotoxins) adhered to the surface of the dust particles thus increasing the harmful effects of dust particles (Palmero et al., 2011). Moreover, during the period of transport to urban or industrial areas, the mineral dust can be mixed with emissions from other sources such as refineries and thermal power stations (Moreno et al., 2010; Rodríguez et al., 2011; Salvador et al., 2016). In addition, it has been suggested that during African dust transport events, the toxicity of PM_{10} of local origin can increase (Pérez et al., 2012b). That is, the same concentration of PM_{10} will have greater effects on health during these types of events than in the other days. This suggests the existence of an interaction or synergy between air pollutants from local sources and the occurrence of African events, with a consequent increase in the risk of mortality due to exposure to them. In this line, Pandolfi et al. (2014) found that African dust episodes were associated with a lowering of the mixing layer (the layer adjacent to the ground available for the dispersion of the pollutants) in Barcelona. This atmospheric effect enhanced local and regional atmospheric pollution from all sources and increased mortality during African dust outbreaks in this study area. The decreasing of the MLH during African dust outbreaks that presumably produced the higher mortality rates at Barcelona has not been evaluated at any other site to date (Staffogia et al., 2016).

This study aims to check the hypothesis proposed by Pandolfi et al. (2014) by evaluating the impact of long-range transport of African dust events of different intensity, on levels of particulate matter, gaseous pollutants, vertical structure of the atmosphere and daily mortality in the Madrid metropolitan area. The exacerbation of dust storms due to a changing climate (Goudie and Middleton, 2006; Miri et al., 2007; NMI, 2013) must be monitored in terms of human health and the environment in order to evaluate partially the influence of climate change on air quality in urban areas in the south of Europe.

It is important to stress that in different European regions, the adding effects of high temperatures reached during heatwaves and exposure to levels of tropospheric O_3 and PM_{10} caused increases in mortality rates due to natural and respiratory causes (De Sario et al., 2013). This kind of interactions suggests a 'climate penalty' (IPCC, 2013). Other types of synergies between air pollutants and the occurrence of other extreme atmospheric events such as dust storms are not as yet well established. Jacob and Winner (2009) recognized that the potential effect of climate change on particulate matter is more complicated and uncertain than for O_3. These authors also pointed to the fact that particulate matter is highly sensitive to mixing layer heights but there is no consensus among models up to now on how this meteorological variable will respond to climate change.

2. Methodology

2.1. Characterization of African dust episodes

A robust procedure based on the daily interpretation of air mass back trajectories and meteorological products was used to identify all the African dust episodic days (AFR days) with impact in the levels of PM_{10} registered in the central region of Spain for the period 2011–2014.

Firstly, back-trajectories of air masses (HYSPLIT: https://www.arl.noaa.gov/hysplit/hysplit/) were computed and interpreted to account for the transport of air masses from north-African deserts. Then, aerosol maps from numerical models (BSC-DREAM8b: https://ess.bsc.es/bsc-dust-daily-forecast; NAAPS-NRL: https://www.nrlmry.navy.mil/aerosol/; SKIRON: http://www.forecast.uoa.gr) and satellite images (Sea-WiFS: http://oceancolor.gsfc.nasa.gov/SeaWiFS/; MODIS: http://modis.gsfc.nasa.gov/) were evaluated, which usually result in the consideration of additional days impacted by dust. Finally, for specific cases in which some doubts arise, meteorological maps were calculated (NCEP/NCAR: https://www.esrl.noaa.gov/psd/data/composites/hour/) to verify the existence of favorable scenarios for the transport of dust. This is a qualitatively way to detect the appearance of African dust plumes over the Madrid Air Basin and assures the identification of almost all the African dust episodes, independently of their intensity (Pey et al., 2013).

Then, a statistical analysis of the time series of PM_{10} levels registered at regional background monitoring sites in this area was applied to quantify the African dust contribution on the PM_{10} daily records. Studies made on the levels of PM_{10} registered at EMEP and other regional background stations in the Iberian Península (Escudero et al., 2007b; Querol et al., 2013) showed that the 30 days moving 40th percentile determined for each day, excluding the African dust episodic days, reproduces rather suitably the regional background levels of the study area during periods with prevailing atmospheric advective conditions (Atlantic, Mediterranean and European). Thus, at regional background monitoring sites, the origin of the PM_{10} levels recorded during these days must be local or regional. Consequently this methodology built on the identification of days with African dust transport and statistical analyses based on the calculation of the 30 days moving 40th percentile for regional background PM_{10} daily concentration time series. This percentile is an indicator of the non-African regional background to be subtracted from the daily PM_{10} levels during African dust outbreaks, and thus allows calculating the daily net African dust contribution.

The feasibility of this method was demonstrated by different approaches in Escudero et al. (2007b) and Viana et al. (2010). Currently, this is one of the official methods recommended by the European Commission for evaluating the occurrence of African dust outbreaks and quantifying the dust contributions (Commission staff working paper, 2011). This procedure estimates the impact of each African dust event on the PM_{10} daily records registered at regional background monitoring sites.

It should be noted that Fernández et al. (2017) classified AFR days in some regions of Spain as a function of the associated dust load obtained with this methodology, with the aim to analyse aerosol optical properties. It was found that as the African dust contribution at ground level in the central area of the Iberian Peninsula was larger, the aerosol optical depth (AOD hereafter) over Madrid was greater as well. Since AOD is a measure of the light extinction produced by aerosols, it means that on average the quantification of mineral dust carried out at ground level with this procedure can be used as a reasonably proxy of the concentration of mineral dust throughout the whole atmospheric vertical column.

In this work, the level of dust contribution was used to categorize the degree of intensity or impact of the African dust event. Hence, the more intense African dust episodic days had associated higher values of dust contribution. Finally, a list of African dust events classified by their intensity was created for subsequent analysis. Here, high and low AFR days (AFR-H and AFR-L, respectively) were defined as AFR days with dust contribution to PM_{10} higher than the 50th percentile and lower or equal than the 50th percentile of the data set, respectively.

2.2. Study of the vertical structure of the atmosphere during African dust episodes

The vertical structure of the atmosphere over Madrid was characterized by means of radiosondes and lidar products. Special attention was paid to the mixing layer height (MLH). The MLH was defined by Seibert et al. (2000) as the height of the layer adjacent to the ground over which pollutants or any constituents emitted within this layer or

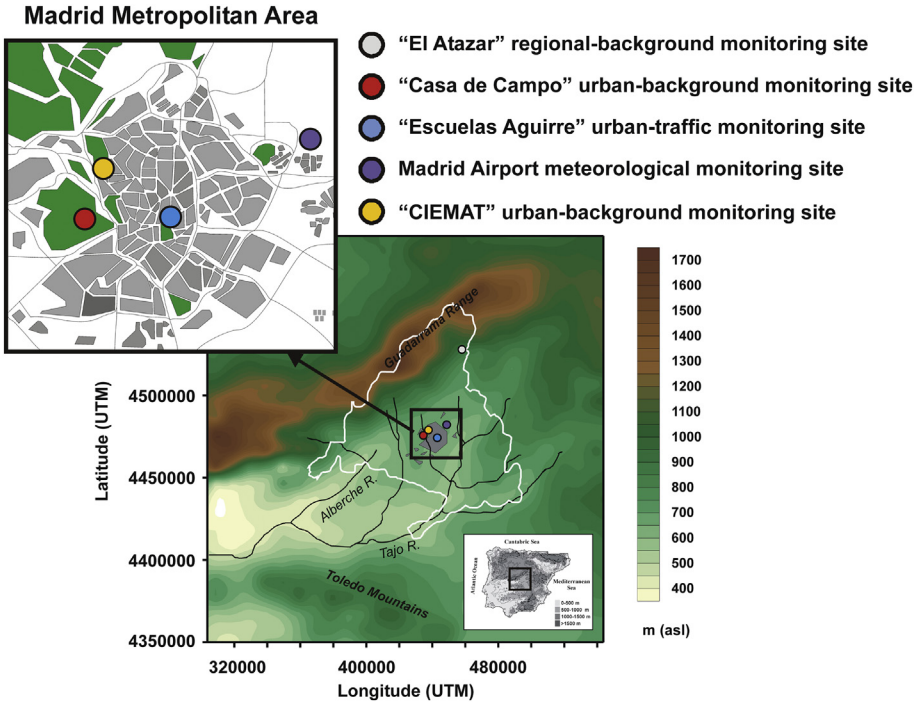

Fig. 1. Geographical location of the different air quality monitoring sites in the Madrid air basin and of the Madrid Airport where radiosondes were carried out.

entrained into it become vertically dispersed by convection or mechanical turbulence within a time scale of about an hour. Thus, the lower the MLH the higher the concentration of air pollutants emitted from local sources in urban areas.

The study of vertical profiles of meteorological variables by means of radiosondes enables estimating the MLH at midday. Radiosondes are launched at 00 and 12 UTC every day at the Madrid airport (40.47°N, 3.56°W, 610 m above sea level - asl, Fig. 1) by the Spanish Meteorological Agency (AEMET). Datasets were available for 94% of the days of the period 2011–2014. They were obtained and analyzed to obtain the midday MLH over Madrid by means of the simple parcel method (Holzworth, 1964). Following this procedure the MLH is taken as the equilibrium level of an air parcel with potential temperature calculated at ground level.

It should be noted that the Madrid airport is located 10 km away from the Madrid city center at the NE direction (Fig. 1). Stability conditions across the Madrid metropolitan area can be slightly different than in the Madrid airport, especially in the Madrid city center due to the well-known urban heat island effect (Yagüe et al., 1991; Salamanca et al., 2012). However, the results obtained in the present work confirmed that levels of air pollutants registered at different air quality monitoring stations in the Madrid metropolitan area fluctuated according to the variations of the MLH determined at the Madrid airport.

On the other hand, lidar is a well-established technique for continuous vertical profiling of aerosols throughout the troposphere with a vertical resolution of a few meters and a temporal resolution in the range of minutes (Baars et al., 2008). CIEMAT lidar station (40.45°N, 3.72°W, 672 m asl, Fig. 1) is based on a multiwavelength Raman lidar instrument that forms part of EARLINET (European Aerosol Reseach lidar NETwork) and consequently performs regular measurements for climatological purposes and fulfilled the protocols established by this network (Pappalardo et al., 2014). The essential characteristics of the CIEMAT lidar system have been described elsewhere (Molero et al., 2014). The main lidar products are the range corrected signal (raw signal multiplied by the squared distance) and the backscatter coefficient. The lidar signal was registered in 1 min integrated time, with vertical resolution of 3.75 m. From the temporally averaged elastic lidar signal, usually 30 min averages, aerosol backscatter coefficient profiles were retrieved using the Klett–Fernald algorithm (Klett, 1981; Fernald, 1984). Both parameters inform qualitatively about the aerosol presence resolved in height. Temperature and pressure profiles provided by radiosonde data launched by nearby Madrid Airport were used to calculate molecular profiles. The retrieval of backscatter coefficient profiles requires the use of an a priori selected value for the lidar ratio (i.e. the ratio between aerosol extinction and backscatter coefficient) that was kept constant at 40 sr. This value is typically used for continental aerosol (Wang et al., 2014). During daytime measurements, the AOD can be obtained by integrating the lidar-derived extinction coefficient profile, obtained by multiplying the backscattering coefficient profiles by the lidar ratio. As the biaxial lidar system does not provide information in the near range due to overlap limitations of the biaxial configuration between the laser beam and the telescope field of view, the backscatter coefficient value in this near range was assumed constant and equal to the first reliable value found at the lowest full-overlap height (~300 m above ground level - agl).

Lidar products thus allow detecting the presence of airborne aerosol strata of different density, observing their evolution and characterizing their properties. In summary, lidar measurements were available for 279 days of the period of study (19% of the total), with 45 corresponding to AFR days but only 28 were carried out at daytime periods, most of them starting around 14:00 h UTC. Only daytime cases were selected in order to consider convectively-driven mixing layers.

2.3. Air pollutants data from air quality monitoring stations

Time series of PM_{10} daily concentrations recorded at "El Atazar" regional background station (40.90°N, 3.46°W, 995 m asl, Fig. 1), were used to quantify the net African dust load transported to the central region of Spain, in any AFR day of the period 2011–2014. This monitoring station belongs to the Madrid Regional Air Quality Network. It is the closest regional background station to the Madrid metropolitan area (~75 km). The values of African dust load were used to classify each AFR day by their intensity.

Next, time series of levels of PM_{10}, $PM_{2.5}$ (the mass of particulate matter which passes through a size selective impactor inlet with a 50% efficiency cut-off at 2.5 μm aerodynamic diameter) and gaseous

pollutants (NO, NO_2 and CO) registered at specific monitoring sites of the Madrid City Air Quality Network were obtained and analyzed with the aim to obtain correlations with the variability of the MLH. One urban-traffic oriented monitoring station located in the center of Madrid ("Escuelas Aguirre", 40.42°N, 3.68°W, 692 m asl, Fig. 1) and another urban-background monitoring site located in a big park in the Madrid outskirts ("Casa de Campo", 40.41°N, 3.74°W, 645 m asl, Fig. 1) were selected. Additionally, time series of daily mean particle number concentrations obtained at the "CIEMAT" urban-background site (40.45°N, 3.72°W, 672 m asl, Fig. 1) with a TSI-SMPS instrument (Wang and Flagan, 1990) were also analyzed. This instrument provides ultrafine particles (UFP) size distributions and number concentrations between 15 and 600 nm. In the Madrid metropolitan area the main local source of primary UFP is traffic (Brines et al., 2015). In the summer period, UFP generated by nucleations can also appear at the regional scale (Carnerero et al., 2018). The nucleation precursor gases can be anthropogenic and biogenic.

Ancillary meteorological information registered at the CIEMAT meteorological tower was also analyzed to evaluate the evolution of different meteorological variables during dust-free days (non-AFR) and AFR days of different intensity. The instrumented tower installed at CIEMAT facilities measures temperature, wind direction and speed at 54 m agl, precipitation and solar radiation at 35 m agl, temperature and humidity at 4 m agl and pressure at ground level. Data were recorded every 10 min. The temperature gradient ΔT was obtained as the difference of simultaneous temperature records at 54 m and 4 m agl. Positive values of this gradient are indicative of stable atmospheric conditions that can be associated to surface thermal inversions.

Afterwards, two additional gridded coefficients that characterize the atmospheric stability near the ground level were obtained using the mathematical routine of the HYSPLIT (HYbrid Single-Particle Lagrangian Integrated Trajectory) transport and dispersion model (Stein et al., 2015). This model combines Lagrangian and Eulerian approaches, considering the air parcels motion from a moving frame of reference and a fixed-three dimensional grid. By using the gridded meteorological data from the ARL (Air Resources Laboratory) database of the NOAA (National Oceanic and Atmospheric Administration), HYSPLIT incorporates several atmospheric stability parameters (Rolph et al., 2017), which characterize the turbulent mixing within the boundary layer from the fluxes of heat and momentum. The subgrid-scale horizontal mixing coefficient (K_h) is computed from the velocity deformation and the vertical mixing coefficient (K_z) from the heat coefficient (Draxler and Hess, 1997 and references therein). These stability variables were daily averaged with the aim to obtain an indicator of the average degree of turbulence during AFR days of different intensity, that could help to interpret the results obtained from radiosondes and the CIEMAT meteorological tower.

With the aim to check the impact of African dust in the daily mean levels of atmospheric pollutants and meteorological parameters registered at the different monitoring sites ("Escuelas Aguirre", "Casa de Campo", "CIEMAT" and Madrid Airport) with statistical significance, the Kolmogorov-Smirnov test was applied. This is one of the most useful and general non-parametric method to perform two samples comparison (Fernández et al., 2017). Tests were performed for the comparison between non-AFR against AFR days and between AFR days of different intensity (AFR-L and AFR-H).

2.4. Short-term effects on daily mortality

We collected daily mortality by all-external causes (International Classification of Diseases, ICD9: 001-799 ICD10 A00-R99) in the Madrid City for the study period between 1st January 2011 and 31st December 2014. It represents daily mortality counts by all the causes excluding those produced by natural causes. Data was obtained from the Spanish Statistical Institute (INE). The association between all-cause mortality and daily measurements of particulate matter was investigated using a case-crossover design that compares exposure at case days (i.e. death) with exposure at days in which the event did not happen (control days) (Jaakkola, 2003). Control days were selected using a time-stratified approach from the same day of the week, month and year as case days (Levy et al., 2001). Data were analyzed using conditional Poisson regression models (Armstrong et al., 2014). We controlled for temperature in the regression models using the averaged temperature on the same day of the exposure day and the day before (averaged lag 0–1), to control for the immediate effects dominated by heat, and the averaged temperature of the second to the fourth days before the exposure (averaged lag 2–4), to control for effects of lower temperatures at longer lags (Pandolfi et al., 2014). Finally, we also controlled for public holidays. The effect modification by AFR days was examined by creating a dummy variable for the presence or absence dust at exposure days and its interaction with the air quality parameters in the regression models. Estimates are reported as the percentage increase in risk of mortality (%IRR), defined as (relative risk − 1) × 100% and its 95% confidence intervals (CIs) for an interquartile range (IQR) increase in the environmental exposure. Analyses were done using Stata, version 14, statistical software (StataCorp, College Station, TX, USA).

3. Results and discussion

3.1. Analysis of time series of gases and particle mass and number concentrations

In the period 2011–2014, 70 African dust outbreaks with impact in the regional background levels of PM_{10} in the centre of the Iberian Peninsula were detected. All these episodes accounted for a total of 214 AFR days. It represents 15% of all the days of the period of study. On average 18 episodes per year (~54 AFR days/year) were identified with a mean duration of 3 AFR days per episode. The number of annual events ranged from 12 in 2013 to 20 in 2011 and 2012. Their duration was very variable, ranging from 1 to 10 days. The annual number of AFR days thus ranged from 39 in 2013 to 64 in 2014. The highest number of African dust events was detected in summer (42.5% of the total, Fig. 2). The occurrence of these episodes was equal in spring and autumn (26.6%) whereas the lowest frequency was obtained for the winter period (4.2%). These results are very similar, in terms of the number of events detected (18 episodes per year), their duration (4 AFR days per episode) and their seasonal evolution (higher frequency of occurrence in the summer period followed by the autumn and spring periods) to those published in Salvador et al. (2013) for the period 2001–2008 in the same area of study.

Mean daily levels of PM_{10}, $PM_{2.5}$ and NO_2 at the urban and the urban-background stations increased during AFR days with respect to non-AFR days in 2011–2014 (Table 1 and Fig. 3a). The most outstanding increase was obtained for PM_{10} levels (87% and 127%, respectively). $PM_{2.5}$ levels also increased but at a lower proportion (58%

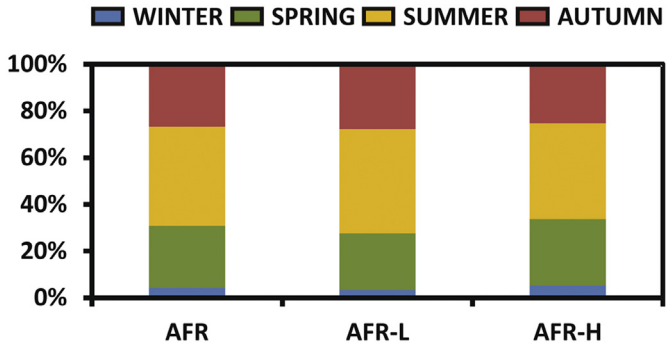

Fig. 2. Seasonal evolution of the occurrence of African dust episodic days over the Madrid air basin in the period 2011–2014.

Table 1
Daily mean values (and standard deviation) of concentrations of atmospheric pollutants registered at the air quality monitoring stations of "Escuelas Aguirre", "Casa de Campo" and "CIEMAT", and meteorological variables at "CIEMAT" and Madrid Airport, during all the days of the period 2011–2014 (ALL), dust-free days (non-AFR), all the African dust episodic days (AFR), and the AFR days of low (AFR-L) and high (AFR-H) intensity.

	ALL	non-AFR	AFR	AFR-L	AFR-H
"Escuelas Aguirre" urban-traffic monitoring site					
PM_{10} (μg/m^3)	25 (15)	23 (11)	42 (19)[a]	34 (10)	53 (23)[b]
$PM_{2.5}$ (μg/m^3)	13 (6)	12 (5)	19 (7)[a]	16 (4)	23 (8)[b]
NO_2 (μg/m^3)	51 (17)	50 (17)	56 (16)[a]	52 (14)	61 (16)[b]
NO (μg/m^3)	32 (31)	33 (32)	27 (22)[a]	23 (20)	32 (23)[b]
CO (mg/m^3)	0.35 (0.16)	0.35 (0.16)	0.34 (0.15)	0.31 (0.13)	0.37 (0.17)[b]
"Casa de Campo" urban-background monitoring site					
PM_{10} (μg/m^3)	18 (12)	15 (7)	34 (20)[a]	25 (7)	45 (26)[b]
$PM_{2.5}$ (μg/m^3)	9 (5)	8 (4)	14 (6)[a]	11 (3)	18 (6)[b]
NO_2 (μg/m^3)	23 (16)	23 (16)	25 (11)[a]	23 (11)	29 (11)[b]
NO (μg/m^3)	9 (16)	10 (17)	7 (9)[a]	6 (9)	8 (9)[b]
CO (mg/m^3)	0.24 (0.09)	0.24 (0.09)	0.23 (0.06)[a]	0.22 (0.06)	0.24 (0.06)[b]
"CIEMAT" urban-background monitoring site					
Number (#/cm^3)	7534 (4389)	7475 (4554)	7894 (3206)	7324 (2525)	8654 (3827)[b]
RAD (W/m^2)	180 (94)	174 (95)	215 (81)[a]	228 (79)	199 (81)[b]
WS (m/s)	4.3 (3.1)	4.4 (3.2)	3.8 (2.3)[a]	4.1 (2.3)	3.4 (2.3)[b]
Rainfall (mm)	0.71 (2.73)	0.75 (2.87)	0.42 (1.72)[a]	0.44 (1.91)	0.39 (1.42)[b]
T (°C)	15.6 (7.8)	14.5 (7.5)	22.2 (5.9)[a]	21.8 (5.5)	22.8 (6.3)[b]
RH (%)	53.6 (20.0)	55.5 (20.0)	42.4 (16.1)[a]	42.6 (15.1)	42.1 (17.5)
ΔT (°C)	0.64 (0.71)	0.65 (0.52)	0.60 (0.74)	0.54 (0.48)	0.67 (0.54)[b]
Madrid Airport meteorological monitoring site					
MLH (m asl)	1572 (553)	1563 (558)	1624 (523)	1743 (523)	1472 (486)[b]

Number: ultra-fine particles number concentration; RAD: surface solar radiation; WS: surface wind speed; Rainfall: daily accumulated precipitation; RH: surface relative humidity; T: surface temperature; ΔT: temperature gradient = temperature at 54 m – temperature at 3.5 m; MLH: mixing layer height at midday.

[a] Statistically significant differences between non-AFR and AFR days at the 95% confidence level.

[b] Statistically significant differences between AFR-L and AFR-H days at the 95% confidence level.

and 70%, respectively). It is well known that in Spain, African dust outbreaks generally produce a higher impact on PM_{10} than on $PM_{2.5}$ levels due to the characteristic coarse size of mineral particles in the range 2.5–10 μm (Querol et al., 2008). NO_2 mean levels rose by 11% and 13% at the "Escuelas Aguirre" and "Casa de Campo" monitoring sites in AFR days, respectively.

Mean concentration of UFP were also slightly higher in AFR than in non-AFR days (6% at the CIEMAT urban-background site) but differences were not statistically significant. Otherwise, CO and NO daily mean values were lower during AFR than in non-AFR days at both sites (4% and 5%, respectively for CO data sets and 11% and 9%, respectively for NO data sets). These differences were rather low in all the cases and even without statistical significance for CO between AFR and non-AFR days.

These results could be partly attributed to the fact that AFR days were more frequently produced during the warmest months of the year (Fig. 2). They were characterized by statistically significant higher solar radiation and temperature than non-AFR days (Table 1 and Fig. 3a). Thus, aside from the external contribution of African dust, photochemical secondary formation of NO_2 from NO was enhanced as a result of the titration reaction with tropospheric O_3. This fact also contributed to reach higher levels of NO_2 in AFR than in non-AFR days.

Unlike them, most non-AFR days in Madrid as in many regions of the Iberian Peninsula (Querol et al., 2004) were characterized by prevailing dispersive conditions (higher mean wind speed and precipitation than in AFR days, Table 1 and Fig. 3a) currently associated to the advection of air masses at the synoptic scale, mainly from N-NW Atlantic regions. Under these unstable atmospheric conditions, the levels of most air pollutants were reduced in the metropolitan area. This effect was evident in the case of the PM_{10}, $PM_{2.5}$ and NO_2 levels whose levels were significantly lower in non-AFR than in AFR days. Unlike these air pollutants, UFP, CO and NO did not decreased significantly during non-AFR days. NO, CO and to a lesser extent UFP (mainly in the winter period, Brines et al., 2015) are good tracers of primary emissions from combustion sources such as road traffic and residential heating that are typically found at metropolitan urban areas such as the Madrid one. They reach their highest levels during the occurrence of the classical urban high-pollution episodes in Madrid (Artíñano et al., 2004; Gómez-Moreno et al., 2011; Salvador et al., 2012; Borge et al., 2018). This type of events is associated to stationary high pressure systems that favor the accumulation of high levels of particles and gaseous pollutants from local sources, mainly in the winter period. These episodic days were classified as non-AFR days. When the daily mean levels of NO, CO and UFP registered during all the non-AFR days were averaged, the low levels associated to the advection of clean air masses were counteracted by the maximum values reached during the urban high-pollution episodes, resulting in similar or even higher mean levels than during AFR days.

When it comes to AFR days of different intensity, 119 AFR-L and 95 AFR-H days were identified in 2011–2014. It should be noted that the same seasonal evolution was obtained for AFR-L, AFR-H and all the AFR days (Fig. 2).

Our results showed that the daily mean levels of PM_{10}, $PM_{2.5}$, NO_2, NO, CO and UFP number concentration significantly increased with stronger AFR days at the Madrid urban and urban-background monitoring stations (Fig. 3b). The Kolmogorov-Smirnov non-parametric test determined that there were statistically significant differences in all the cases between the distributions at the 95% confidence level (Table 1). The comparison of the mean levels of local meteorological variables indicated that AFR-H days were characterized by lower values of solar radiation, wind speed and precipitation close to the ground than AFR-L days (Table 1 and Fig. 3b). These results suggested that AFR-H days occurred under more stable atmospheric conditions than AFR-L days. The mean daily values of the temperature gradient at the CIEMAT monitoring site were also significantly higher in AFR-H than in AFR-L days (Table 1 and Fig. 3b). The average daily evolution of the hourly values of this temperature gradient showed in Fig. 4, insinuate the development of stronger nocturnal thermal inversions in AFR-H than in AFR-L days. When the dust load during AFR days was subtracted from the daily mean PM_{10} values registered at the urban and urban-background monitoring sites, we could obtain an estimation of the contribution of the urban sources to these levels in the area around these sites. This urban contribution was higher on average in AFR than in non-AFR days, 34% at the urban and 47% the urban-background sites. It should also be noted that the urban contribution increased in AFR-H days with respect to AFR-L days (13% and 28% μg/m^3 at "Escuelas Aguirre" and "Casa de Campo", respectively). It can be interpreted that the contribution of local sources of particles and gaseous pollutants also increased during the AFR days of highest intensity due to the relatively stronger stability conditions.

3.2. Mixing layer height characterization during African dust episodic days

Regarding the MLH estimations, a total of 1375 values were determined for the period 2011–2014 with the simple parcel method. 211 out of them corresponded to AFR days which cover 99% of all AFR days detected. When the impact of African dust on the mixing layer

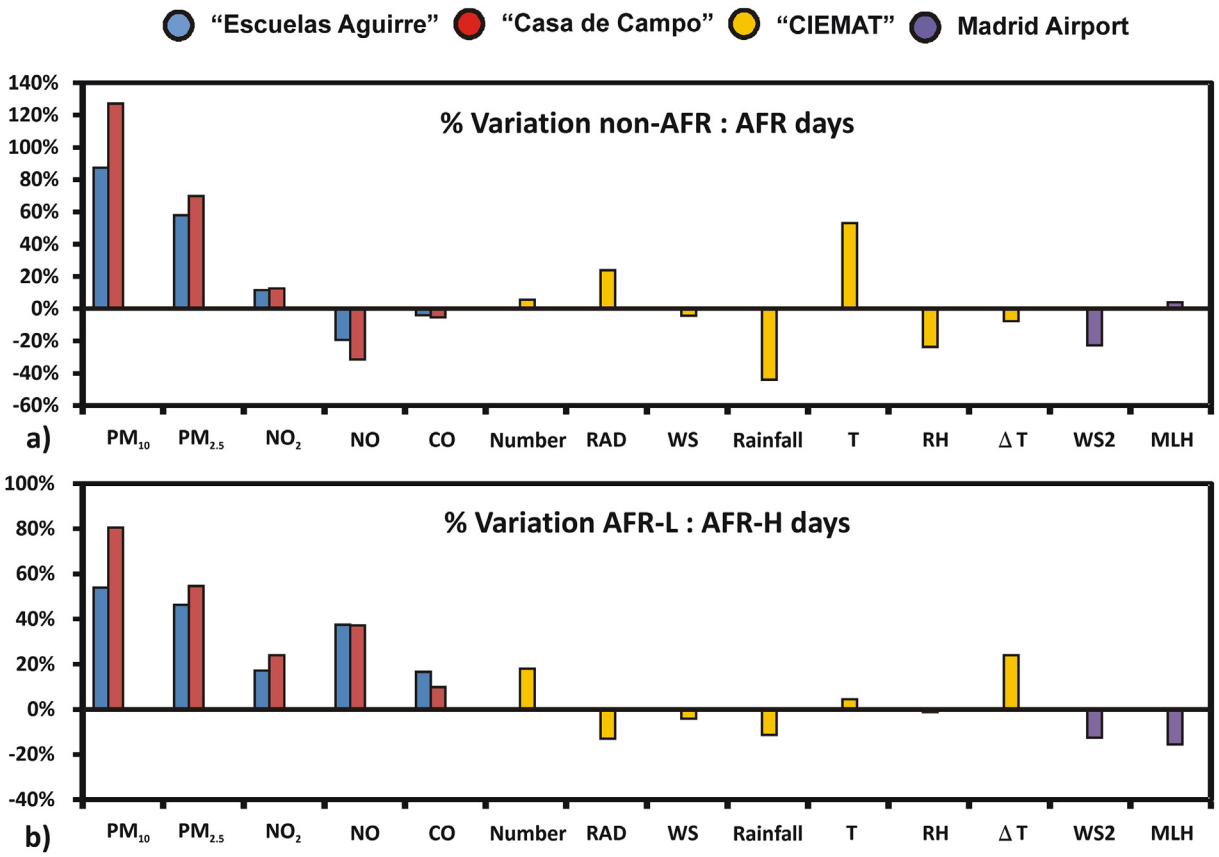

Fig. 3. Variability (increase or reduction) in daily mean values of atmospheric pollutants and meteorological variables from dust-free days (non-AFR) to African dust episodic days (AFR) (a) and from African dust episodic days of low intensity (AFR-L) to high intensity (AFR-H), expressed as percentages. Number: ultra-fine particles number concentration; RAD: surface solar radiation; WS: surface wind speed; Rainfall: daily accumulated precipitation; T: surface temperature; RH: surface relative humidity; ΔT: temperature gradient = temperature at 54 m – temperature at 3.5 m; MLH: mixing layer height at midday.

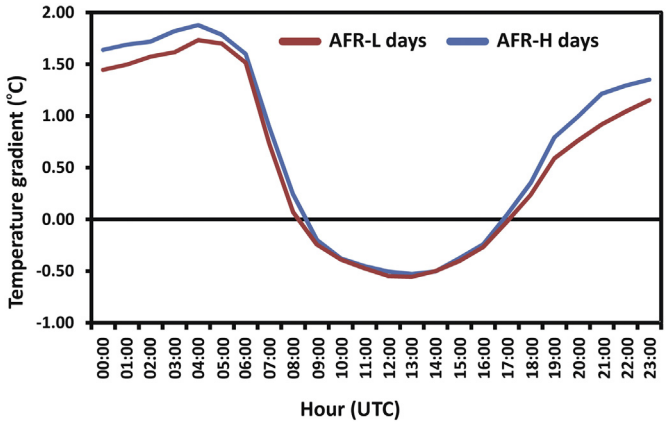

Fig. 4. Average daily evolution of the hourly values of the temperature gradient obtained from temperature records performed at 54 m and 3.5 m at CIEMAT during African dust episodic days of low (AFR-L) and high (AFR-H) intensity.

evolution was checked, radiosounding data taken at midday indicated that there were not statistically significant differences at the 95% confidence level between MLH values on AFR and non-AFR days (Table 1). Otherwise, the MLH significantly decreased with increasing intensity of the AFR days (Table 1 and Fig. 5a). A mean reduction of 16% of MLH (271 m) was observed from AFR-L to AFR-H days (Fig. 3b). The MLH reduction was detected across all the year but it was slightly higher in absolute values in the spring (280 m - mean reduction of 16%) and the summer (277 m - 14%) months than in the autumn (229 m - 15%) and the winter (219 m - 21%) months.

Fig. 6 shows two examples of the evolution of aerosol layers observed in the lidar measurements in AFR-H days. The left panels show the temporal evolution of the range-corrected lidar signals at 532 nm. And the right panels, the backscatter coefficient profiles at the three elastic wavelengths (355, 532 & 1064 nm) calculated by averaging the three 15-min time periods highlighted in the left panels. In the first case (17-Aug-2012), an aerosol-rich layer was observed from ground up to 5 km, but inside this layer, the lowering of a higher backscattering coefficient layer was detected. The second case (26-Jul-2012), the aloft layer, located between 4 and 6 km, suffers a lowering towards ground levels and starts to affect the mixing layer at the end of the measurements. These two cases exemplify the phenomenon attributed to the increase in ground-level pollutant concentration, as the lidar measurements were classified into 2 different groups: Those characterized by the identification of a single aerosol layer above ground (such as the first case, comprising 54% of the data) and another group of measurements that showed an upper aerosol layer above that (46%). For both groups of data, it was frequently detected the lowering along the measurement periods of either layers of high concentration of aerosols near the ground or the upper aerosol layers. On the other hand, the short-time measurements, one hour period, of the lidar data prevent a better characterization of the phenomenon. These measurements are programmed for climatological studies within the EARLINET protocol. Further investigation can be undertaken in the future, characterizing the evolution of the African dust intrusions along the whole duration of the event.

Fig. 7 shows the averaged vertical profiles of the backscattering coefficient during AFR-L and AFR-H days, obtained from lidar measurements in the period 2011–2014. The values of this parameter near the surface were higher during AFR-H days than in the other episodic

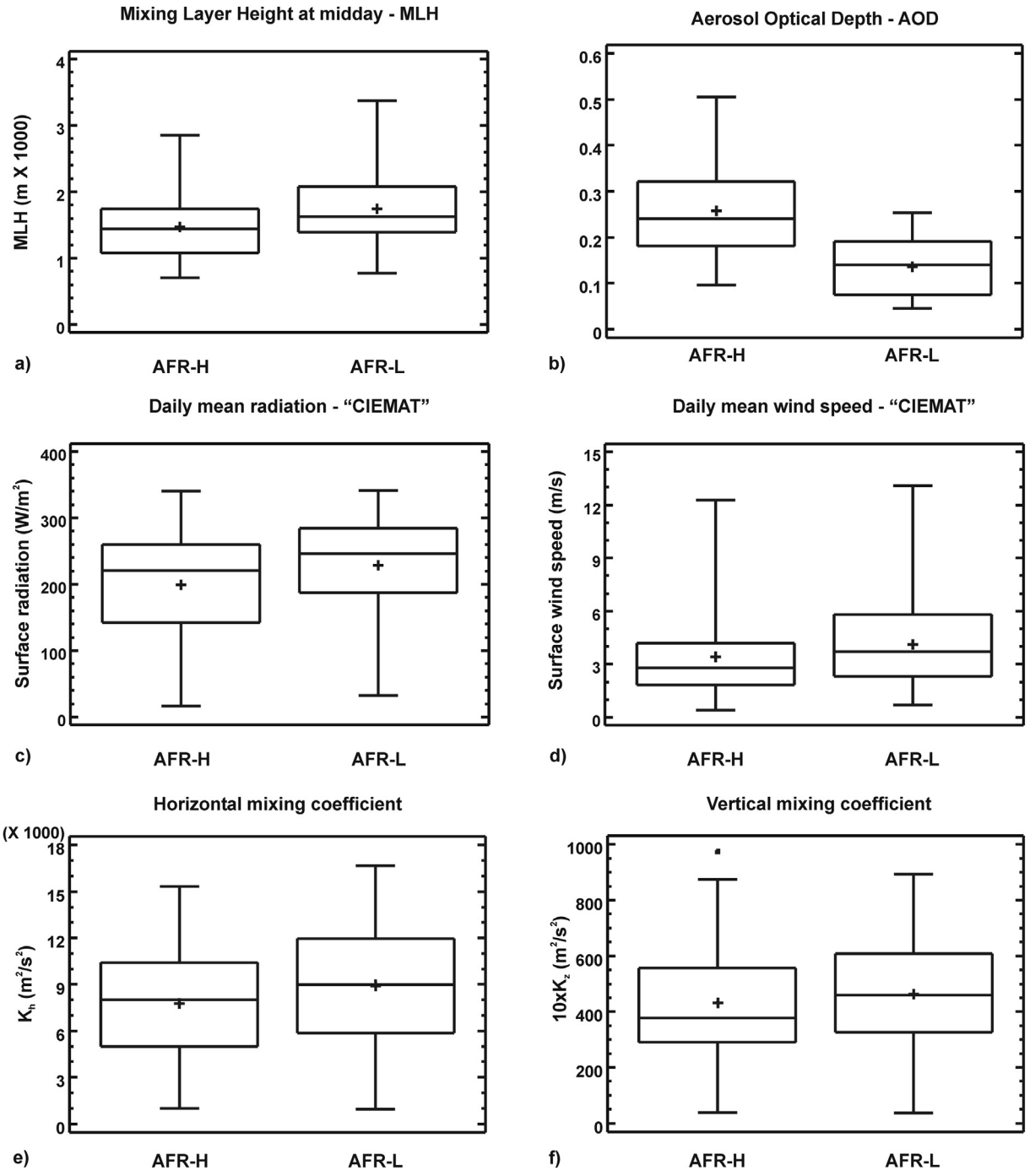

Fig. 5. Boxplots of mixing layer height at midday-MLH over Madrid (a), aerosol optical depth-AOD (b), daily mean radiation at surface level (c), daily mean wind speed at surface (d), horizontal mixing coefficient (e) and vertical mixing coefficient (f) during African dust episodic days of low (AFR-L) and high (AFR-H) intensity. Mean value of the data set is represented by the cross. Median is drawn as a horizontal line inside the box.

days. It means that the higher the intensity of the AFR day the higher the aerosol concentration detected by the lidar in the low troposphere. Besides, Fig. 5b illustrates that AFR-H days presented a higher mean AOD value (0.258) than AFR-L (0.136) in good agreement with the results of Fernández et al. (2017). Solar radiation also decreased progressively (30 W/m^2) from AFR-L to AFR-H days (Table 1 and Fig. 5c). Statistically significant differences between the distributions were obtained in all the cases for a 95% confidence level (Table 1). These results can be interpreted as follows. The lower solar radiation reaching surface during AFR days of increasing intensities (Fig. 5c), limited the convective growth of the mixing layer over Madrid. Other studies have highlighted this kind of interaction between aerosols and the mixing layer. Li et al. (2017 and references therein) stated that both aerosol scattering and absorption substantially reduced the amount of solar radiation reaching the ground and thus reduced the sensible heat fluxes that drive the diurnal evolution of the mixing layer in many regions of Asia.

It should also be considered that in the absence of significant air mass advection at the synoptic scale, regional wind circulations are responsible of air pollutants dispersion in the Madrid air basin. The daily cycle of slope heating and cooling of the Guadarrama mountain range (Fig. 1) acts as the main driving force of this type of thermally

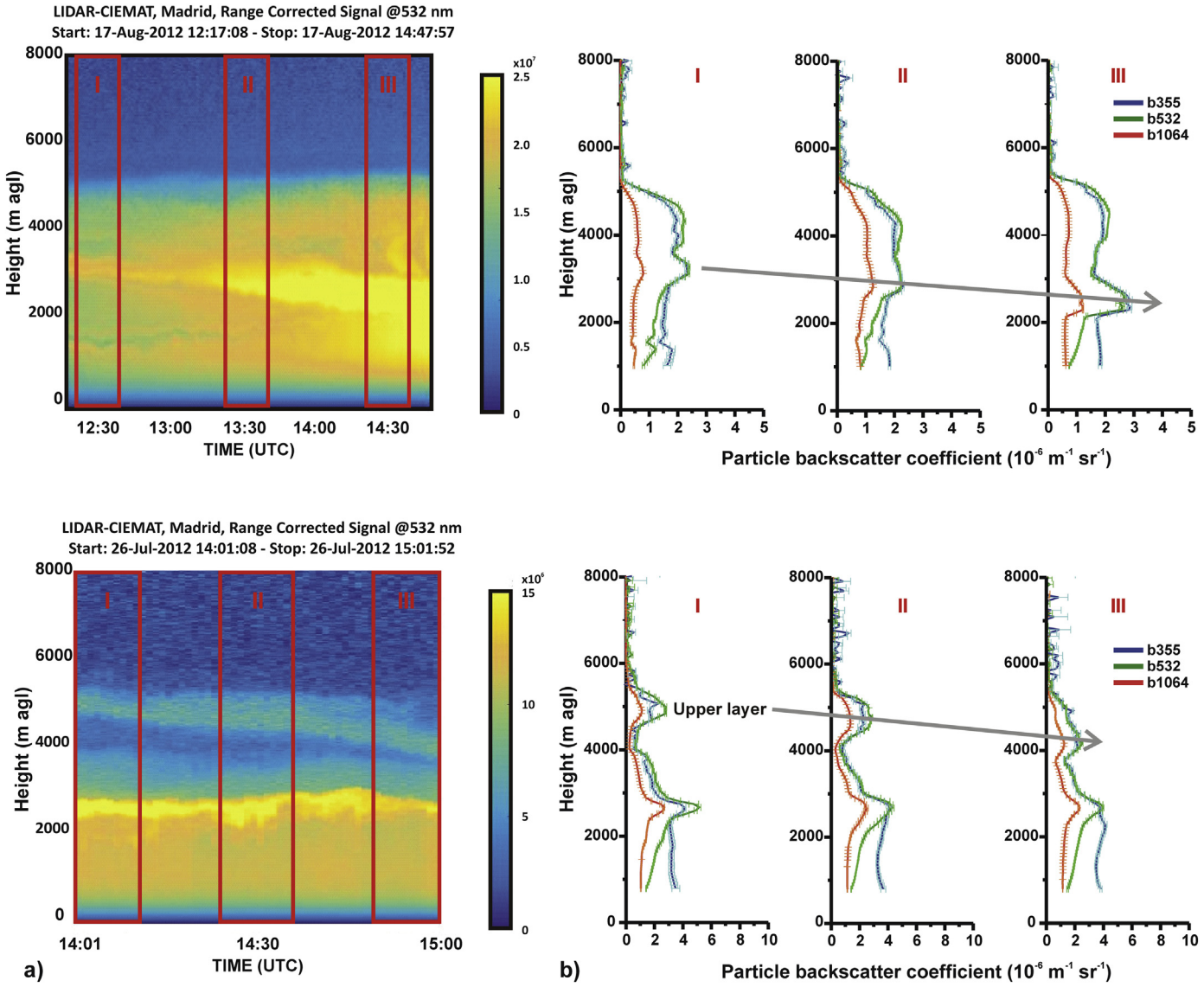

Fig. 6. Range corrected signal values derived on 17-Aug-2012 (up) and 26-Jul-2012 (down) at 532 nm (a). Backscatter coefficient profiles (at 355, 532 and 1064 nm) retrieved for three 15 min periods (b). Grey arrows show the lowering of highly concentrated aerosol layers towards the ground.

induced circulations in this air basin (Plaza et al., 1997). Their intensity is thus, also modulated by incoming solar radiation. During the sampling period, horizontal wind speed at surface also decreased progressively from AFR-L to AFR-H days (0.7 m/s) with statistical significance (Fig. 5d). This was probably a consequence of the lower solar radiation and the prevailing stable conditions observed during AFR-H days, since the daily mean values of the horizontal and vertical mixing coefficients also decreased from AFR-L to AFR-H days (Fig. 5e–f).

Hence, the increase of the levels of NO_x, CO and UFP in Madrid during AFR-H days (Fig. 3b) could be attributed to the progressive accumulation of emissions from local sources in the reduced distribution atmospheric volume and to the reduced wind speed produced close to the ground. Borge et al. (2018) analised in detail an urban high-pollution episode produced in Madrid on December 2016. They found a close relationship between the reduced MLH registered at midday along all the days of the episode and the high levels of NO_2 registered at the urban air quality monitoring stations located across the urban metropolitan area. The usefulness of the MLH in air pollution issues was highlighted by these authors who proposed to use the inversion base height computed from vertical temperature soundings, as an index to anticipate favorable atmospheric conditions leading to urban high-pollution episodes and trigger the application of a short term air quality action plan in Madrid.

3.3. Association between PM_{10} and $PM_{2.5}$ and daily mortality in AFR days

The short-term effects of particulate matter were examined at different lags, up to 4 days. The strongest effects were observed at lags 1 and 2 and are reported below. Statistically significant associations of PM_{10} and $PM_{2.5}$ with all-cause mortality were observed for AFR and non-AFR days (Fig. 8). However, the %IRR for an IQR increase in the PM_{10} exposure was higher for AFR (2.2%, 95%CI = [0.3; 4.1]; IQR = 20 μg/m^3) than for non-AFR days (1.6%, 95%CI = [0.6; 2.7]; IQR = 15 μg/m^3). Similar values of %IRR were obtained for $PM_{2.5}$ for both AFR and non-AFR days (1.3, 95%CI = [−0.3; 3.0]; IQR = 7 μg/m^3 and 1.2%, 95%CI = [0.4; 1.9]; IQR = 5 μg/m^3). These results are in good agreement with a similar study carried out for the Madrid area during the period 2003–2005 (Tobías et al., 2011).

Moreover, we have found evidence of stronger adverse health effects of PM_{10} during AFR days of increasing intensity with the conditional Poisson regression models (Fig. 9). The IRR calculated for PM_{10} concentrations were higher in AFR-H than in AFR-L days and ranged

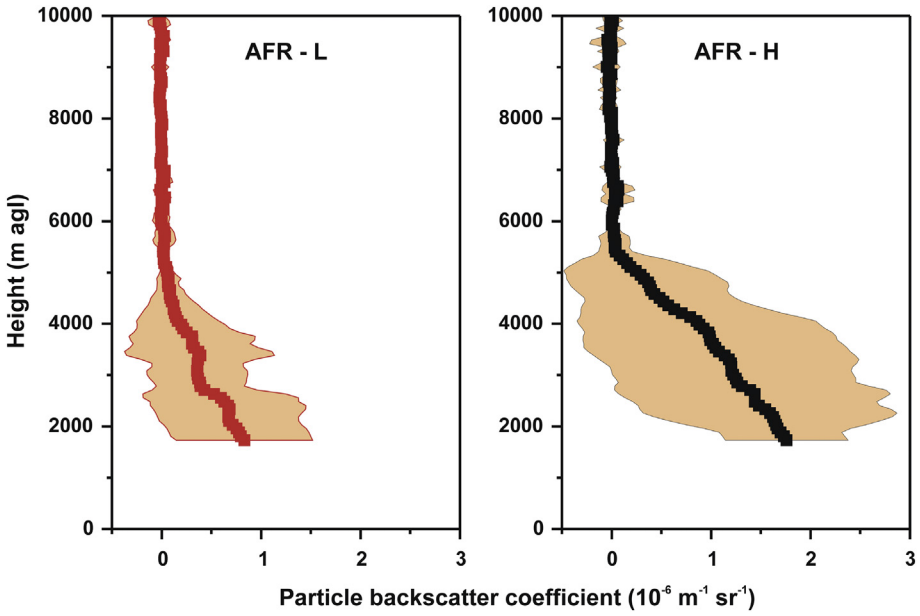

Fig. 7. Mean particle backscatter coefficient profiles at 532 nm obtained averaging profiles obtained during African dust episodic days of low (AFR-L) and high (AFR-H) intensity (Mean: black and red squares; Standard deviation: orange shade). Data were missing below 1800 m agl for some profiles due to technical problems during the measurements. (For interpretation of the references to colour in this figure legend, the reader is referred to the web version of this article.)

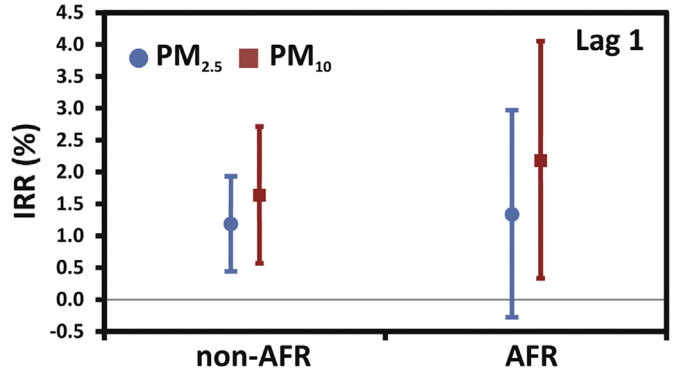

Fig. 8. Percentage increases in risk of mortality (%IRR) for an interquartile range increase in the environmental exposure to PM_{10} and $PM_{2.5}$ during dust-free days (non-AFR) and African dust episodic days (AFR) in 2011–2014.

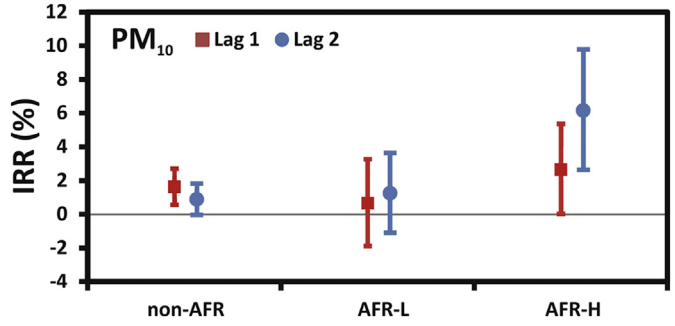

Fig. 9. Percentage increases in risk of mortality (%IRR) for an interquartile range increase in the environmental exposure to PM_{10} during dust-free days (non-AFR) and African dust episodic days of low (AFR-L) and high (AFR-H) intensity in 2011–2014.

from 2.7% (95%CI = [0.02; 5.36]; IQR = 24 μg/m^3) for lag 1 to 6.2% (95%CI = [2.6; 9.8]; IQR = 24 μg/m^3) for lag 2 (Fig. 9). Regarding AFR-L days the association with daily mortality for both lags were not statistically significant. Hence, it can be concluded that adverse effects on daily mortality produced during AFR days in Madrid were produced when the dust contribution exceeded a threshold value (i.e. from AFR-L to AFR-H events, 8 μg/m^3). It reflects a higher toxicity of the same concentration of PM_{10} in AFR-H days with lower mixing height days than on AFR-L days when MLH were higher. The observed increased concentrations of local pollution ($PM_{2.5}$, gaseous compounds from road traffic emissions and UFP) with decreasing MLH in the Madrid metropolitan area may favor the formation of specific relevant particulate matter species likely from condensation of accumulated gaseous precursors on the surface of dust particles and/or formation of new fine particles. These processes can take some time to happen. This could be the reason why adverse effects were stronger 2 days after the AFR-H day happened.

Hence, it can be concluded that the same atmospheric effect that Pandolfi et al. (2014) described for the Barcelona metropolitan area in 2003–2010 was detected in Madrid in 2011–2014, in relation with the fact that AFR days caused a reduction of MLH with consequent accumulation of man-made local pollutants. It also contributed to increase harmful effects on health of PM_{10} during AFR days of high intensity at both sites.

It should be stressed that the evolution of the mixing layer is different at a Mediterranean coastal site such as Barcelona than at a continental site in the centre of the Iberian Peninsula such as Madrid. In the Mediterranean borderline of Spain, the mixing layer evolution is highly controlled by the strong geographical gradients of height and the development of sea breezes (Millán et al., 1991; Sicard et al., 2006). Over Madrid the development of the MLH further depends on the convective turbulence that is higher in the summer period, when incoming radiation is stronger than in the other seasons (Crespí et al., 1995). Otherwise, strong high pressure conditions with weak gradient pressure at surface during the winter months, favor the formation of surface-based inversions during the night and shallow MLH during the day, leading also to very weak winds near surface and high NO_2 levels in Madrid (Borge et al., 2018).

The identification of the same synergistic effect at sites like Madrid and Barcelona with complex mixing layer dynamics, lead to consider that it could also happen in other urban sites of the Mediterranean basin that are under the influence of frequent African dust outbreaks (Querol et al., 2009; Pey et al., 2013; Staffogia et al., 2016).

4. Conclusions

African dust episodes of high intensity were associated with a lowering of the mixing layer height over Madrid. The concentration of high levels of dust close to the ground during African dust episodic days

of increasing intensity seems to be responsible for mixing layer height narrowing. For this reason PM_{10} levels increased due to the contribution of mineral dust but also to the accumulation of PM_{10} emissions from local sources in the reduced mixing layer. Furthermore, African dust episodes increased the concentrations of other atmospheric pollutants that may potentially affect human health and the environment. It can be concluded that ambient air in Madrid was more toxic during African dust episodic days of increasing intensity due to this synergistic effect. Hence, with the aim to reduce harmful effects on human health, selected measures should be implemented during the occurrence of African dust outbreaks, for abating air pollution emissions from local anthropogenic sources. Measures should probably be similar to those carried out during severe urban air pollution episodes that frequently happen in the Madrid metropolitan area, under stable meteorological conditions (Borge et al., 2018).

Future investigations are required to fully characterize these results, since the exacerbation of events of long-range transport of dust from arid regions, as predicted in some changing climate scenarios (IPCC, 2013) will impact on exceedances of air quality standards and human health. An increase in the frequency of dust storms has been detected in numerous desert regions of the Sahara and Sahel during the second half of the 20th century as a result of high temperatures, the decrease in precipitations associated with an increase in periods of drought, and increased soil erosion caused by anthropogenic factors (Goudie and Middleton, 2006). Recently published papers have voiced the opinion that tropics are expanding towards the pole in both hemispheres (Heffernan, 2016) and that Sahara desert has expanded significantly over the 20th century (Thomas and Nigam, 2018) towards the Sahel region and the northern borderline of Africa (10% on average in 1920–2013). These regions have been identified by Ginoux et al. (2012) as recent “anthropogenic non-hydro” dust source areas.

The identification of an interaction or synergy between the air pollution levels to which the population in Madrid is exposed and the occurrence of events of African dust outbreaks, has enabled partial assessment of the influence of climate change on air quality in urban areas in the south of Europe and consequent adverse health effects on the population.

Acknowledgements

This work was funded by research projects SINERGIA (CA_CC16) with the support of the “Biodiversity Foundation” from the Spanish Ministry for the Ecological Transition (MITECO) and CRISOL (CGL2017-85344-R) under the Spanish Ministry of Economy and Competitiveness (MINECO) Research and Innovation Plan.

The authors wish to thank the NOAA Air Resources Laboratory (ARL) for the provision of the HYSPLIT trajectory model. We also acknowledge the Atmospheric Modelling & Weather Forecasting Group in the University of Athens, the Earth Science Dpt. from the Barcelona Supercomputing Centre, the Naval Research Laboratory and the SeaWiFS project (NASA) for the provision of the SKIRON, DREAM/BSC-DREAM8b, NAAPs aerosol maps, and the satellite imagery, respectively.

References

Armstrong, B.G., Gasparrini, A., Tobias, A., 2014. Conditional Poisson models: a flexible alternative to conditional logistic case cross-over analysis. BMC Med. Res. Methodol. 14, 122. https://doi.org/10.1186/1471-2288-14-122.

Artíñano, B., Salvador, P., Alonso, D.G., Querol, X., Alastuey, A., 2004. Influence of traffic on the PM_{10} and $PM_{2.5}$ urban aerosol fractions in Madrid (Spain). Sci. Total Environ. 334-335, 111–123.

Baars, H., Ansmann, A., Engelmann, R., Althausen, D., 2008. Continuous monitoring of the boundary-layer top with lidar. Atmos. Chem. Phys. 8, 7281–7296.

Borge, R., Artíñano, B., Yagüe, C., Gomez-Moreno, F.J., Saiz-Lopez, A., Sastre, M., Narros, A., García-Nieto, D., Benavent, N., Maqueda, G., Barreiro, M., de Andrés, J.M., Cristóbal, A., 2018. Application of a short term air quality action plan in Madrid (Spain) under a high-pollution episode - part I: Diagnostic and analysis from observations. Sci. Total Environ. 635, 1561–1573.

Brines, M., Dall'Osto, M., Beddows, D.C.S., Harrison, R.M., Gómez-Moreno, F., Núñez, L., Artíñano, B., Costabile, F., Gobbi, G.P., Salimi, F., Morawska, L., Sioutas, C., Querol, X., 2015. Traffic and nucleation events as main sources of ultrafine particles. Atmos. Chem. Phys. 15, 5929–5945.

Carnerero, C., Pérez, N., Reche, C., Ealo, M., Titos, G., Lee, H., Eun, H., Park, Y., Dada, L., Paasonen, P., Kerminen, V., Mantilla, E., Escudero, M., Gómez-Moreno, F.J., Alonso-Blanco, E., Coz, E., Saiz-Lopez, A., Temime-Roussel, B., Marchand, N., Beddows, D.C.S., Harrison, R.M., Petäjä, T., Kulmala, M., Ahn, K., Alastuey, A., Querol, X., 2018. Vertical and horizontal distribution of regional new particle formation events in Madrid. Atmos. Chem. Phys. 18, 16601–16618.

Commission Staff Working Paper, 2011. Establishing Guidelines for Demonstration and Subtraction of Exceedances Attributable to Natural Sources under the Directive 2008/50/EC on Ambient Air Quality and Cleaner Air for Europe, Brussels, 15.02.2011. SEC(2011) 208 Final. 37 pp., available at: http://ec.europa.eu/environment/air/quality/legislation/pdf/sec_2011_0208.pdf (last access February 2019).

Crespí, S.N., Artíñano, B., Cabal, H., 1995. Synoptic clasification of the Mixed-Layer height evolution. J. Appl. Meteorol. 34 (7), 1666–1676.

De Sario, M., Katsouyanni, K., Michelozzi, P., 2013. Climate change, extreme weather events, air pollution and respiratory health in Europe. Eur. Respir. J. 42 (3), 826–843. https://doi.org/10.1183/09031936.00074712.

Díaz, J., Linares, C., Carmona, R., Russo, A., Ortiz, C., Salvador, P., Machado Trigo, R., 2017. Saharan dust intrusions in Spain: Health impacts and associated synoptic conditions. Environ. Res. 156, 455–467.

Draxler, R.R., Hess, G., 1997. Description of the HYSPLIT_4 modelling system. In: NOAA Tech. Mem. ERL ARL-224, Scientific Report, pp. 28. available at. https://www.arl.noaa.gov/documents/reports/arl-224.pdf (last access February 2019).

Escudero, M., Querol, X., Ávila, A., Cuevas, E., 2007a. Origin of the exceedances of the European daily PM limit value in regional background areas of Spain. Atmos. Environ. 41, 730–744.

Escudero, M., Querol, X., Pey, J., Alastuey, A., Pérez, N., Ferreira, F., Cuevas, E., Rodríguez, S., Alonso, S., 2007b. A methodology for the quantification of the net African dust load in air quality monitoring networks. Atmos. Environ. 41, 5516–5524.

Fernald, F.G., 1984. Analysis of atmospheric Lidar observations - some comments. Appl. Opt. 23 (5), 652–653.

Fernández, A.J., Molero, F., Salvador, P., Revuelta, A., Becerril-Valle, M., Gómez-Moreno, F.J., Artíñano, B., Pujadas, M., 2017. Aerosol optical, microphysical and radiative forcing properties during variable intensity African dust events in the Iberian Peninsula. Atmos. Res. 196, 129–141.

Ginoux, P., Prospero, J.M., Gill, T.E., Hsu, N.C., Zhao, M., 2012. Global-scale attribution of anthropogenic and natural dust sources and their emission rates based on MODIS Deep Blue aerosol products. Rev. Geophys. 50, RG3005. https://doi.org/10.1029/2012RG000388.

Gómez-Moreno, F.J., Pujadas, M., Plaza, J., Rodríguez-Maroto, J.J., Martínez-Lozano, P., Artíñano, B., 2011. Influence of seasonal factors on the atmospheric particle number concentration and size distribution in Madrid. Atmos. Environ. 45, 3169–3180.

Goudie, A.S., Middleton, N.J., 2006. Desert Dust in the Global System. ISBN-10 3-540-32354-6. Springer (287 pp.).

Heffernan, O., 2016. The mystery of the expanding tropics. Nature 530, 20–22.

Holzworth, C.G., 1964. Estimates of mean maximum mixing depths in the contiguous United States. Mon. Weather Rev. 92, 235–242.

IPCC, 2013. Climate change 2013: the physical science basis. In: Stocker, T.F., Qin, D., Plattner, G.-K., Tignor, M., Allen, S.K., Boschung, J., Nauels, A., Xia, Y., Bex, V., Midgley, P.M. (Eds.), Contribution of Working Group I to the Fifth Assessment Report of the Intergovernmental Panel on Climate Change. Cambridge University Press, Cambridge, United Kingdom and New York, NY, USA (1535 pp.).

Jaakkola, J.J., 2003. Case-crossover design in air pollution epidemiology. Eur. Respir. J. 21 (40), 81–85.

Jacob, D.J., Winner, D.A., 2009. Effect of climate change on air quality. Atmos. Environ. 43, 51–63.

Klett, J.D., 1981. Stable analytical inversion solution for processing lidar returns. Appl. Opt. 20 (2), 211–220.

Levy, D., Lumley, T., Sheppard, L., Kaufman, J., Checkoway, H., 2001. Referent selection in case-crossover analyses of acute health effects of air pollution. Epidemiology 12, 186–192.

Li, Z., Guo, J., Ding, A., Liao, H., Liu, J., Sun, Y., Wang, T., Xue, H., Zhang, H., Zhu, B., 2017. Aerosol and boundary-layer interactions and impact on air quality. Nat. Sci. Rev. 4 (6), 810–833. https://doi.org/10.1093/nsr/nwx117.

Millán, M.M., Artíñano, B., Alonso, L., Navazo, M., Castro, M., 1991. The effect of meso-scale flows on regional and long-range atmospheric transport in the Western Mediterranean area. Atmos. Environ. 25A (5/6), 949–963.

Miri, A., Ahmadi, H., Ghanbari, A., Moghaddamnia, A., 2007. Dust storms impacts on air pollution and public health under hot and dry climate. Int. J. Energy Environ. 1 (2), 101–105.

Molero, F., Andrey, F.J., Fernandez, A.J., Parrondo, M.C., Pujadas, M., Cordoba-Jabonero, C., Revuelta, M.A., Gomez-Moreno, F.J., 2014. Study of vertically resolved aerosol properties over an urban background site in Madrid (Spain). Int. J. Remote Sens. 35 (6), 2311–2326.

Moreno, T., Pérez, N., Querol, X., Amato, F., Alastuey, A., Bhatia, R., Spiro, B., Hanvey, M., Gibbons, W., 2010. Physicochemical variations in atmospheric aerosols recorded at sea onboard the Atlantic-Mediterranean 2008 Scholar Ship cruise (Part II): natural versus anthropogenic influences revealed by PM10 trace element geochemistry. Atmos. Environ. 44, 2563–2576.

Moulin, C., Lambert, C.E., Dulac, F., Dayan, U., 1997. Control of atmospheric export of

dust from North Africa by the North Atlantic Oscillation. Nature 387, 691–694.
Moulin, C., Lambert, C.E., Dayan, U., Masson, V., Ramonet, M., Bousquet, P., Legrand, M., Balkanski, Y.J., Guellel, W., Marticorena, B., Bergametti, G., Dulac, F., 1998. Satellite climatology of African dust transport in the Mediterranean atmosphere. J. Geophys. Res. 103, 13137–13144.
NMI, 2013. Extreme Weather Events in Europe: Preparing for Climate Change Adaptation. Norwegian Academy of Science and Letters and the Norwegian Meteorological Institute, Oslo Scientific Report, 140 pp., available at: http://www.dnva.no/binfil/download.php?tid=58783 (last access February 2019).
Palmero, D., Rodríguez, J.M., de Cara, M., Camacho, F., Iglesias, C., Tello, J.C., 2011. Fungal microbiota from rain water and pathogenicity of Fusarium species isolated from atmospheric dust and rainfall dust. J. Ind. Microbiol. Biotechnol. 38, 13–20. https://doi.org/10.1007/s10295-010-0831-5.
Pandolfi, M., Tobias, A., Alastuey, A., Sunyer, J., Schwartz, J., Lorente, J., Pey, J., Querol, X., 2014. Effect of atmospheric mixing layer depth variations on urban air quality and daily mortality during Saharan dust outbreaks. Sci. Total Environ. 494, 283–289.
Pappalardo, G., Amodeo, A., Apituley, A., Comerón, A., Freudenthaler, V., Linné, H., Ansmann, A., Bösenberg, J., D'Amico, G., Mattis, I., Mona, L., Wandinger, U., Amiridis, V., Alados-Arboledas, L., Nicolae, D., Wiegner, M., 2014. EARLINET: towards an advanced sustainable European aerosol lidar network. Atmos. Meas. Tech. 7, 2389–2409.
Pérez, L., Tobías, A., Querol, X., Pey, J., Alastuey, A., Díaz, J., Sunyer, J., 2012a. Saharan dust, particulate matter and cause specific mortality: a Case-Crossover study in Barcelona (Spain). Environ. Int. 48, 150–155.
Pérez, L., Tobías, A., Pey, J., Pérez, N., Alastuey, A., Sunyer, J., Querol, X., 2012b. Effects of local and Saharan particles on cardiovascular disease mortality. Epidemiology 23, 768–769.
Pey, J., Querol, X., Alastuey, A., Forastiere, F., Stafoggia, M., 2013. African dust outbreaks over the Mediterranean Basin during 2001–2011: PM10 concentrations, phenomenology and trends, and its relation with synoptic and mesoscale meteorology. Atmos. Chem. Phys. 13, 1395–1410.
Plaza, J., Pujadas, M., Artíñano, B., 1997. Formation and transport of the Madrid ozone plume. J. Air Waste Manag. Assoc. 47, 766–774.
Prospero, J.M., Lamb, P.J., 2003. African droughts and dust transport to the Caribbean: climate change implications. Science 302, 1024–1027.
Querol, X., Alastuey, A., Puicercus, J.A., Mantilla, E., Miro, J.V., Lopez-Soler, A., Plana, F., Artíñano, B., 1998. Seasonal evolution of suspended particles around a large coal-fired power station: particulate levels and sources. Atmos. Environ. 32, 1963–1978.
Querol, X., Alastuey, A., Rodríguez, S., Viana, M.M., Artíñano, B., Salvador, P., Mantilla, E., García do Santos, S., Fernández Patier, R., de la Rosa, J., Sanchez de la Campa, A., Menéndez, M., 2004. Levels of PM in rural, urban and industrial sites in Spain. Sci. Total Environ. 334-335, 359–376.
Querol, X., Alastuey, A., Moreno, T., Viana, M., Castillo, S., Pey, J., Rodríguez, S., Artíñano, B., Salvador, P., Sánchez, M., Garcia Dos Santos, S., Herce Garraleta, M., Fernandez-Patier, R., Moreno-Grau, S., Negral, L., Minguillón, M., Monfort, E., Sanz, M., Palomo-Marín, R., Pinilla, E., Cuevas, E., de la Rosa, J., Sánchez de la Campa, A., 2008. Spatial and temporal variations in air borne particulate matter (PM10 and PM2.5) across Spain 1999–2005. Atmos. Environ. 42 (17), 3964–3979.
Querol, X., Alastuey, A., Pey, J., Pandolfi, M., Cusack, M., Pérez, N., Viana, M., Moreno, T., Mihalopoulos, N., Kallos, G., Kleanthous, S., 2009. African dust contributions to mean ambient PM10 mass-levels across the Mediterranean Basin. Atmos. Environ. 43 (28), 4266–4277.
Querol, X., Alastuey, A., Pey, J., Escudero, M., Castillo, S., Orío, A., González, A., Pallarés, M., Jiménez, S., Ferreira, F., Marques, F., Monjardino, J., Cuevas, E., Alonso, S., Artíñano, B., Salvador, P., de la Rosa, J., 2013. Procedimiento para identificación de episodios naturales africanos de PM_{10} y $PM_{2.5}$, y la demostración de causa en lo referente a las superaciones del valor límite diario de PM_{10}. Sci. Rep. 1, 40. available at. https://www.miteco.gob.es/es/calidad-y-evaluacion-ambiental/temas/atmosfera-y-calidad-del-aire/metodologiaparaepisodiosnaturales-revabril2013_tcm30-186522.pdf (last access February 2019).
Rodríguez, S., Alastuey, A., Alonso-Pérez, S., Querol, X., Cuevas, E., Abreu-Afonso, J., Viana, M., Pérez, N., Pandolfi, M., de la Rosa, J., 2011. Transport of desert dust mixed with North African industrial pollutants in the subtropical Saharan air layer. Atmos. Chem. Phys. 11, 6663–6685.
Rolph, G., Stein, A., Stunder, B., 2017. Real-time environmental applications and display system: ready. Environ. Model Softw. 95, 210–228.
Salamanca, F., Martilli, A., Yagüe, C., 2012. A numerical study of the urban Heat Island over Madrid during the DESIREX (2008) campaign with WRF and an evaluation of simple mitigation strategies. Int. J. Climatol. 32, 2372–2386.
Salvador, P., Artíñano, B., Viana, M., Alastuey, A., Querol, X., 2012. Evaluation of the changes in the Madrid metropolitan area influencing air quality: analysis of 1999-2008 temporal trend of particulate matter. Atmos. Environ. 57, 175–185.
Salvador, P., Artíñano, B., Molero, F., Viana, M., Pey, J., Alastuey, A., Querol, X., 2013. African dust contribution to ambient aerosol levels across central Spain: characterization of long-range transport episodes of desert dust. Atmos. Res. 127, 117–129.
Salvador, P., Alonso, S., Pey, J., Artíñano, B., de Bustos, J.J., Alastuey, A., Querol, X., 2014. African dust outbreaks over the western Mediterranean basin: 11 year characterization of atmospheric circulation patterns and dust source areas. Atmos. Chem. Phys. 14, 6759–6775. https://doi.org/10.5194/acp-14-6759-2014.
Salvador, P., Almeida, S.M., Cardoso, J., Almeida-Silva, M., Nunes, T., Cerqueira, M., Alves, C., Reis, M.A., Chaves, P.C., Artíñano, B., Pio, C., 2016. Composition and origin of PM10 in Cape Verde: characterization of long-range transport episodes. Atmos. Environ. 127, 326–339.
Seibert, P., Beyrich, F., Gryning, S., Joffre, S., Rasmussen, A., Tercier, P., 2000. Review and intercomparison of operational methods for the determination of the mixing height. Atmos. Environ. 34, 1001–1027.
Sicard, M., Pérez, C., Rocadenbosch, F., Baldasano, J.M., García-Vizcaino, D., 2006. Mixed-layer depth determination in the Barcelona coastal area from regular lidar measurements: methods, results and limitation. Bound.-Layer Meteorol. 119, 135–157.
Stafoggia, M., the MED-PARTICLES Study Group, 2016. Desert dust outbreaks in Southern Europe: contribution to daily PM_{10} concentrations and short-term associations with mortality and hospital admissions. Environ. Health Perspect. 124, 413–419.
Stein, A.F., Draxler, R.R., Rolph, G.D., Stunder, B.J.B., Cohen, M.D., Ngan, F., 2015. NOAA's HYSPLIT atmospheric transport and dispersion modelling system. Bull. Am. Meteorol. Soc. 96, 2059–2077.
Thomas, T., Nigam, S., 2018. Twentieth-century climate change over Africa: seasonal hydroclimate trends and Sahara desert expansion. J. Clim. 31, 3349–3370.
Tobías, A., Pérez, L., Díaz, J., Linares, C., Pey, J., Alastruey, A., Querol, X., 2011. Short-term effects of particulate matter on total mortality during Saharan dust outbreaks: a case-crossover analysis in Madrid (Spain). Sci. Total Environ. 412–413, 386–389.
Viana, M., Salvador, P., Artíñano, B., Querol, X., Alastuey, A., Pey, J., Latz, A., Cabañas, M., Moreno, T., García, S., Herce-Garraleta, D., Diez, P., Romero, D., Fernandez-Patier, R., 2010. Assessing the performance of methods to detect and quantify African dust in airborne particulates. Environ. Sci. Technol. 44, 8814–8820.
Wang, S.C., Flagan, R.C., 1990. Scanning electrical mobility spectrometer. Aerosol Sci. Technol. 13, 230–240.
Wang, Y., Sartelet, K.N., Bocquet, M., Chazette, P., Sicard, M., D'Amico, G., Léon, J.F., Alados-Arboledas, L., Amodeo, A., Augustin, P., Bach, J., Belegante, L., Binietoglou, I., Bush, X., Comerón, A., Delbarre, H., García-Vízcaino, D., Guerrero-Rascado, J.L., Hervo, M., Iarlori, M., Kokkalis, P., Lange, D., Molero, F., Montoux, N., Muñoz, A., Muñoz, C., Nicolae, D., Papayannis, A., Pappalardo, G., Preissler, J., Rizi, V., Rocadenbosch, F., Sellegri, K., Wagner, F., Dulac, F., 2014. Assimilation of lidar signals: application to aerosol forecasting in the western Mediterranean basin. Atmos. Chem. Phys. 14, 12031–12053.
Yagüe, C., Zurita, E., Martínez, A., 1991. Statistical analysis of the Madrid urban heat island. Atmos. Environ. 25B, 327–332.